The effect of the rotational excitation of NO on the stereodynamics for the reaction C (^{3}P) + NO ($X^2\Pi$) →CN ($X^2\Sigma^+$) + O (^{3}P)*

Ma Jian-Jun(马建军)†, Zou Yong(邹 勇), and Liu Hou-Tong(刘厚通)

Department of Applied Physics, Anhui University of Technology, Maanshan 243002, *China*

(Received 6 October 2012; revised manuscript received 10 December 2012)

The stereodynamic properties of the reaction C (^{3}P) + NO($X^2\Pi$) →CN ($X^2\Sigma^+$) + O (^{3}P) in different rotational states of reactant NO are studied theoretically by using the quasiclassical trajectory method on $^2A''$ and $^2A'$ potential energy surfaces (PESs) at a collision energy of 0.06 eV. The vector properties in different rotational states on the two surfaces are discussed in detail. The results indicate that the rotational excitation of NO has considerable influence on the stereodynamic property of the reaction occurring on the two surfaces. At the same time, the calculated polarization-dependent differential cross sections (PDDCSs) in different initial rotational states manifest that products are strongly polarized at three scattering angles.

Keywords: quasiclassical trajectory, vector correlation, rotational excitation

PACS: 34.50.Lf, 82.20.Kh **DOI:** 10.1088/1674-1056/22/6/063402

1. Introduction

In recent years, increasing environmental awareness has focused attention on a variety of undesirable combustion pollutants. The gas-phase reactions of atomic carbon with NO,

$$\mathrm{C}\ (^3\mathrm{P}) + \mathrm{NO}(\mathrm{X}^2\Pi) \rightarrow \mathrm{CN}(\mathrm{X}^2\Sigma^+) + \mathrm{O}(^3\mathrm{P}), \quad (1)$$

$$\mathrm{C}\ (^3\mathrm{P}) + \mathrm{NO}(\mathrm{X}^2\Pi) \rightarrow \mathrm{CO}(\mathrm{X}^1\Sigma^+) + \mathrm{N}(^2\mathrm{D}), \quad (2)$$

have received much attention experimentally[1–7] and theoretically,[8–25] owing to their importance in combustion and the interstellar medium, especially for the understanding of NO reburning at high temperatures. The three-atom CNO reactive system exhibits a surprisingly rich chemistry and has many interesting properties.[20] Firstly, it contains fairly few electrons, which makes extensive high-quality quantum chemical calculations affordable. Secondly, two distinct chemical products are formed with different probabilities, on structural grounds, reaction (1) will be the dominant channel because C atoms are more likely to be attracted to the valence electron of the N atom in NO and form the transition complex, CNO*, and reaction (2) is likely to occur by a rearrangement according to the transition state theory.[5] Finally, there is a deep potential well on the surface and the linear intermediates (CNO, NCO, CON) in the ground electronic state $^2\Pi$ are Renner–Teller molecules, the $^2A''$ and $^2A'$ surfaces are degenerate for linear configurations. Quantum dynamical calculations are demanded for the CNO system due to the deep potential wells and the occurrence of three heavy atoms.

The experimental studies of this reaction mainly involve the CN product energy partitioning ro-vibrational distributions and determination of total rate coefficient and the reaction cross section. Krause[1] investigated this reaction in a beam-cell configuration. From the redistribution of total available energy observed, they concluded that the reaction appears to proceed via a "direct" mode rather than "complex" formation. While Naulin *et al.*[4] studied this reaction with pulsed, crossed, supersonic, molecular beams at relative translational energies of 0.06 eV and 0.23 eV. Based on the experiment evidence that the population of distributions shows being definitely non-statistical and the CN recoil-angle distribution appears to be non-isotropic (forward peaked), they drew a conclusion that the reaction proceeds via a pseudo-direct process rather than the complex-mode proposed by Sekiya *et al.*[3]

The theoretical work on this reaction was initiated by Halvick *et al.*,[8–11] who began with an *ab initio* study of the CNO intermediate and the reaction pathways on multiple potential energy surfaces (PESs), and presented that the anisotropy of the intermediate well is an important factor in governing the final distribution of the energy. Wallin *et al.*[12,13] statistically simulated the vibrational and rotational excitation and energy disposal in the crossed beam experiments of Naulin *et al.*[4] Simonson *et al.*[15] and Persson *et al.*[16] used *ab initio* molecular orbital theory to probe the energies of a wide range of configurations of the CNO system, attempted to take the global PES into account, i.e., to include both product channels and all intermediates, and presented a new many-body expansion fit of the $^2A''$ surface associated with the reaction of C + NO. Comparisons between the crossed molecular beam results and the trajectory calculated reaction rate coefficients for both channels indicated that the reaction proceeds via a long-lived complex. Recently, Abrol *et al.*[22] performed wave packet calculations for the collinear

*Project supported by the National Natural Science Foundation of China (Grant No. 41075027).

†Corresponding author. E-mail: mjjdlut@163.com

© 2013 Chinese Physical Society and IOP Publishing Ltd

C + NO reaction, and observed that the dynamical resonances are very sensitive to features of the potential energy surface. More recently, Andersson *et al.*[20,21] presented a new fit of both the $^2A''$ and $^2A'$ surfaces based on additional *ab initio* points for non-linear geometries and a long-range contribution corresponding to electrostatic, induction, and dispersion forces, producing a more realistic analytic representation of the ground state PES. Using the two surfaces, they performed quasiclassical trajectory (QCT) calculations to simulate the crossed molecular beam experiments of Naulin *et al.*,[4] and also calculated the thermal rate coefficients separately for the $^2A''$ and $^2A'$ surfaces in a temperature range from 5 K to 5000 K, which shows that the calculation results are in good agreement with experimental results.[23]

As far as we know, the existing work on the C + NO reaction mainly focuses on the study of scalar property, such as energy distributions, rovibrational populations, and angular distributions for the O + CN product channel, while there is little theoretical and experimental information about the vector properties of this reaction, except for our preliminary work.[25] In this paper we further focus our attention on the influence of rotational excitation of reagent NO on the reaction stereodynamics.

2. Computational method

In this paper, we employ the standard QCT method (see Refs. [26]–[48] and the references therein) and stereodynamics QCT software developed by Han *et al.*[31,35,38–40] Since the stereodynamics theory used here is the same as that in our previous work,[41,42] only the details relevant to the current work are summarized as follows.

The classical Hamilton's equations are numerically integrated in three dimensions. The PESs used in this work are those published in Ref. [20] for the $^2A''$ state, in Ref. [21] for the $^2A'$ state. We do not consider the possible formation of CO and the formation of CN via the $^4\Pi$ surface. These problems will be addressed in future studies. The collision energies are chosen to be 0.06 eV for the two PESs. The vibrational and rotational levels of the reactant molecule are taken as $v = 0$, and $j = 0 \sim 3$, respectively. In the calculation, batches of 2×10^4 trajectories are run for each initial condition, the trajectories are started at a C(^{3}P)–NO distance of 11.0 Å (1 Å = 0.1 nm) and a time step of 0.1 fs is used for the integration of the equations of motion.

3. Results and discussion

The calculated distributions of $P(\theta_r)$ on the $^2A''$ and $^2A'$ PESs for four reagent rotational states (j = 0–3) are shown in Fig. 1. Both figures 1(a) and 1(b) present that the distributions of $P(\theta_r)$ peak at $\theta_r = 90^\circ$ and are symmetric with respect to 90°, which indicates that the product rotational angular momentum vector $\boldsymbol{j}'$ is strongly aligned along the direction perpendicular to the relative velocity vector $\boldsymbol{k}$. Moreover, the peaks of $P(\theta_r)$ become lower and broader as the rotational quantum number increases, meaning that the product rotational alignment effect becomes obviously weaker with the increase of the value of j. Similar results have also been found in reactions of O(^{3}P) + H_2[47,48] and N(^{2}D) + H_2.[49] This may be explained from the expectation values of $\langle P_2(\cos\theta_r)\rangle$ which are −0.1716 (−0.2134), −0.1357 (−0.1808), −0.1171 (−0.1600), and −0.0981 (−0.1345), respectively, herein, the values in the brackets correspond to those on the $^2A'$ PES. $\langle P_2(\cos\theta_r)\rangle$ values are close to −0.5, which suggests that $\boldsymbol{j}'$ is preferentially polarized and perpendicular to the reagent relative velocity. Generally speaking, the well in the PES can lead to a weak product rotational alignment effect, because it may induce "loss" of memory for the angular momentum alignment in that the separation of the products will take various directions in space.[40] The intermediate wells on the two PESs are an important factor in governing the vector properties of reaction. And the rotational excitations of the reagent NO may further increase the isotropic distribution of product rotational angular momentum vector, which weakens the product polarization.

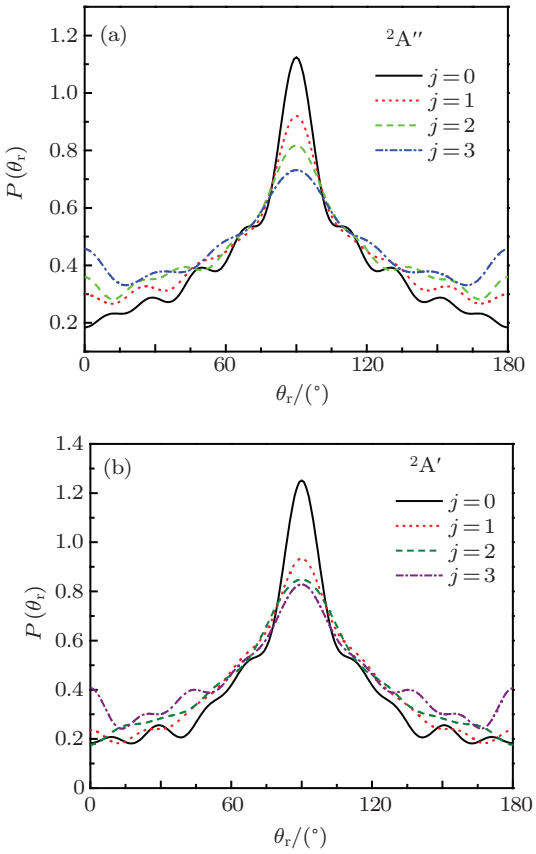


Fig. 1. (color online) Distributions of $P(\theta_r)$ reflecting the $\boldsymbol{k}$–$\boldsymbol{j}'$ correlation at the collision energy of 0.06 eV for the four reagent rotational states, based on the $^2A''$ PES (a) and the $^2A'$ PES (b).

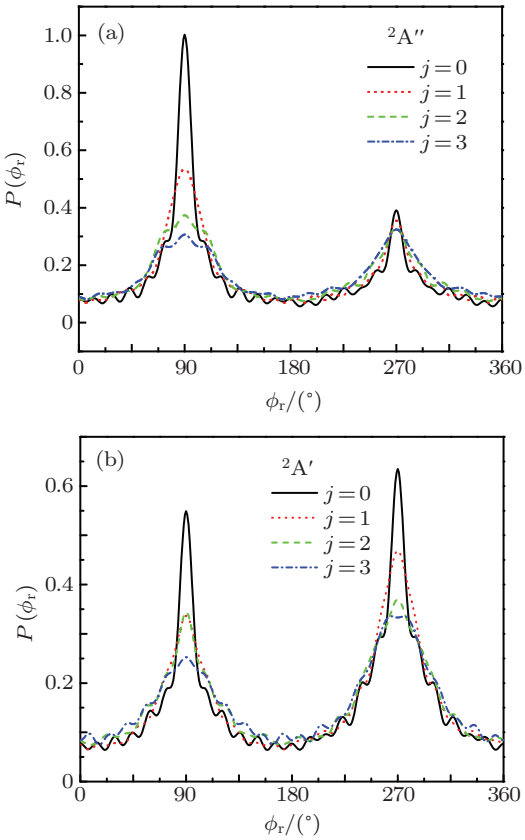


Fig. 2. (color online) Dihedral angle distributions of $P(\phi_r)$ with respect to the $\boldsymbol{k}$–$\boldsymbol{k}'$ plane at the collision energy of 0.06 eV for the four reagent rotational states, based on the ^{2}A″ PES (a) and the ^{2}A′ PES (b).

The dihedral angular distributions of $P(\phi_r)$ shown in Fig. 2 describe the $\boldsymbol{k}$–$\boldsymbol{k}'$–$\boldsymbol{j}'$ correlations. Both figures 2(a) and 2(b) indicate that the distributions of $P(\phi_r)$ tend to be asymmetric with respect to the $\boldsymbol{k}$–$\boldsymbol{k}'$ scattering plane. The peaks of $P(\phi_r)$ appear at $\phi_r = 90°$ and 270°, respectively, and the peaks at $\phi_r = 90°$ are not equal to those at $\phi_r = 270°$, meaning that the angular momentum vector $\boldsymbol{j}'$ is not only aligned, but also oriented along the y axis. The orientation degree of angular momentum $\boldsymbol{j}'$ depends sensitively on the initial rotational state of reactant. As shown in Fig. 2(a), for reaction occurring on the ^{2}A″ PES, as the value of j increases, the peak at $\phi_r = 90°$ tends to become obviously weaker and broader while that at $\phi_r = 270°$ becomes slightly weaker and broader. When $j = 0$, the angular momentum $\boldsymbol{j}'$ is preferentially oriented along the positive direction of y axis. And as the j increases, the $\boldsymbol{j}'$ tends to be oriented along the negative direction of y axis. While for that occurring on the ^{2}A′ PES, Fig. 2(b) shows that all the peaks at $\phi_r = 90°$ are slightly lower than those at $\phi_r = 270°$ for the four different initial rotational excitations of reactant, which implies that the product lightly tends to be oriented along to $-y$ axis (i.e., it prefers the left-handed product rotation in planes parallel to the scattering plane). On both PESs, the peaks at both $\phi_r = 90°$ and $\phi_r = 270°$ become lower and broader with the increase of j, indicating that the product rotational polarization is weaker and the product molecule rotation preferentially changes from the in-plane reaction mechanism to the out-of-plane mechanism at the same time.[46] The asymmetric distributions of $P(\phi_r)$ observed can be explained by the impulse model.[50,51] In the chemical-bond forming and breaking processes in the reaction, the preference for the direction influenced by the repulsive energy between atom N and O will lead to the preferred orientation of the product's angular momentum. In addition, the reagent rotational excitation weakens the repulsive energy, which is the most likely reason why the product alignment and orientation becomes weaker at higher rotational excitation levels.[49]

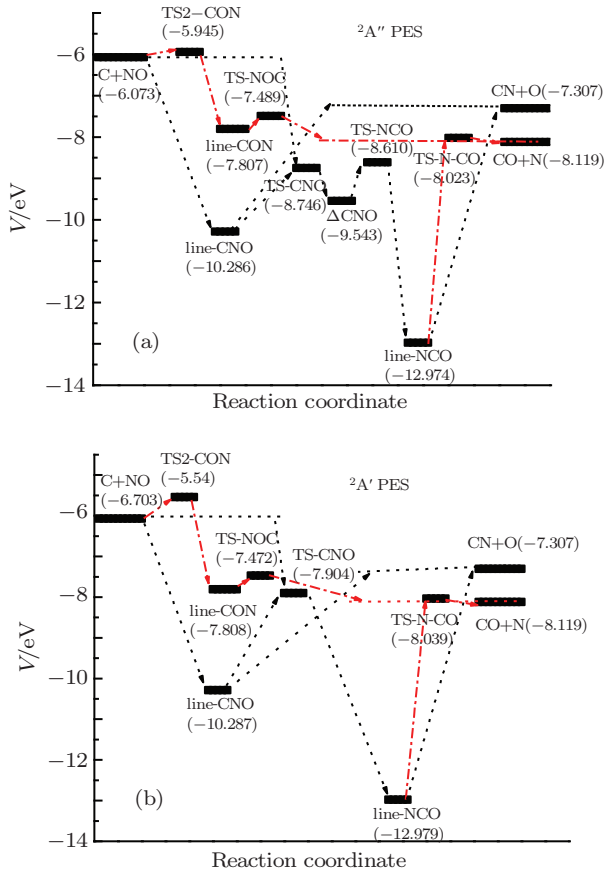


Fig. 3. (color online) Minimum energy paths connecting the reactants (C (^{3}P) + NO ($X^2\Pi$)) with the two sets of the products (CN ($X^2\Sigma^+$) + O (^{3}P), CO ($X^1\Sigma^+$) + N (^{2}D)) via potential minima and transition states. The energies are relative to separated atoms, based on the ^{2}A″ surface (a) and the ^{2}A′ surface (b). Reference data are cited from Refs. [20] and [21]. The dash–dot line are related to the product channel CO ($X^1\Sigma^+$) + N (^{2}D).

The difference in the distribution of $P(\phi_r)$ between on both PESs with the reagent rotational excitations can be ascribed to the difference in structure between the two PESs. The minimum energy paths connecting the reactants (C (^{3}P) + NO ($X^2\Pi$)) with the two sets of the products (CN ($X^2\Sigma^+$) + O (^{3}P), CO ($X^1\Sigma^+$) + N (^{2}D)) are shown in Fig. 3. We can easily see from Fig. 3 that the major difference between the ^{2}A″ and ^{2}A′ surfaces lies in the presence of the triangular minimum (Δ-

CNO) and nonlinear transition state NCO on the $^2A''$ surfaces. Besides, in regions close to the linear minima (CNO, CON, NCO), the $^2A'$ surface slightly is lower in energy than the $^2A''$ surface. For the nonlinear stationary points on both PESs, due to an effect of the triangle minimum Δ-CNO, potential profiles for the different angles of approach of C to NO demonstrate the difference between the surfaces. In long range and for geometries not corresponding to the linear minima (such as transition state TS-CNO), the situation is reversed (i.e., the $^2A''$ surface slightly is lower in energy than the $^2A'$ surface), and all of them will have an important influence on reaction stereodynamics.

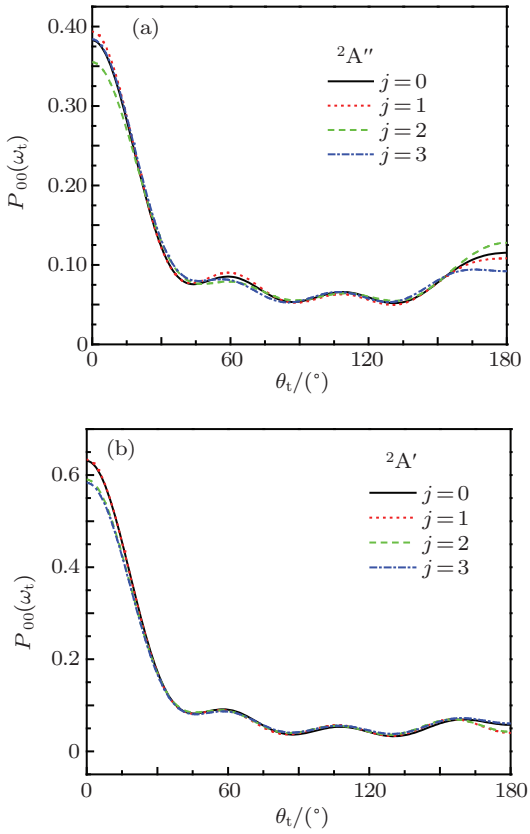


Fig. 4. (color online) Plots of PDDCS $P_{00}(\omega_t)$ versus θ_t for four reagent rotational excitations at a collision energy of 0.06 eV, based on the $^2A''$ PES (a) and the $^2A'$ PES (b).

The polarization-dependent differential cross sections (PDDCSs) can be used to describe the correlation of $\boldsymbol{k}$–$\boldsymbol{k}'$–$\boldsymbol{j}'$ and the scattering direction of the product molecule. Several PDDCSs ($P_{00}(\omega_t)$, $\tilde{P}_{20}(\omega_t)\tilde{P}_{22+}(\omega_t)$) calculated on the two PESs are depict in Figs. 4–6. The distribution of $P_{00}(\omega_t)$ is simply proportional to the differential cross section, and only describes the $\boldsymbol{k}$–$\boldsymbol{k}'$ correlation or the scattering direction of the product. As shown in Fig. 4, the product molecule is scattered strongly forward on either PESs for different initial rotational levels, which is coincident with the experiment results detected by Naulin *et al.*[4] The distributions of the renormalized PDDCS $\tilde{P}_{20}(\omega_t)$ are drawn in Fig. 5, which are related to the expected value $\langle P_2(\cos\theta_r)\rangle$. We can see from the distributions of $\tilde{P}_{20}(\omega_t)$ that the $\boldsymbol{j}'$ is preferentially polarized along the direction perpendicular to $\boldsymbol{k}$ at $\theta_t = 0^\circ$ and 180° for each of four reagent rotation states. The values of all $\tilde{P}_{kq\pm}(\omega_t)$ with $q \neq 0$ are equal to zero at $\theta_t = 0^\circ$ and 180°. The values of $\tilde{P}_{22+}(\omega_t)$ are related to $\langle \sin^2\theta_r \cos 2\phi_r \rangle$. From Fig. 6, it is easy to see that the values of $\tilde{P}_{22+}(\omega_t)$ are negative at all scattering angles, which indicates the marked preference of product alignment along the y axis. More interestingly, we notice that at the scattering angles close to 40°, 85°, and 131°, the products are strongly polarized, which, as mentioned in our previous paper,[25] may be considered to be related with three different transition states (CNO, NCO, CON) existing in the C + NO entrance channel.[20,21] When the scattering angle is near the bond angle which is energetically the most favorable for reaction, the alignment of $\boldsymbol{j}'$ along $\boldsymbol{k}'$ is greatest.[25,51] From Figs. 5 and 6, we can easily note that the degrees of product polarization become weaker with the value of j increasing, which is consistent with the change tendency of distributions of $P(\theta_r)$ and $P(\phi_r)$ with j. Further experimental and theoretical work is still necessary for better understanding its reaction dynamics.

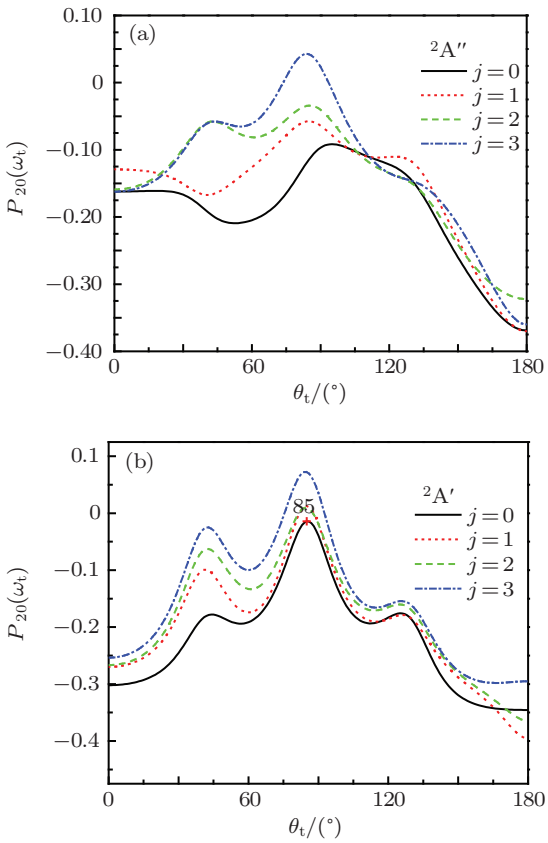


Fig. 5. (color online) Plots of PDDCSs $\tilde{P}_{20}(\omega_t)$ versus θ_t for four reagent rotational excitations at the collision energy of 0.06 eV, based on the $^2A''$ PES (a) and the $^2A'$ PES (b).

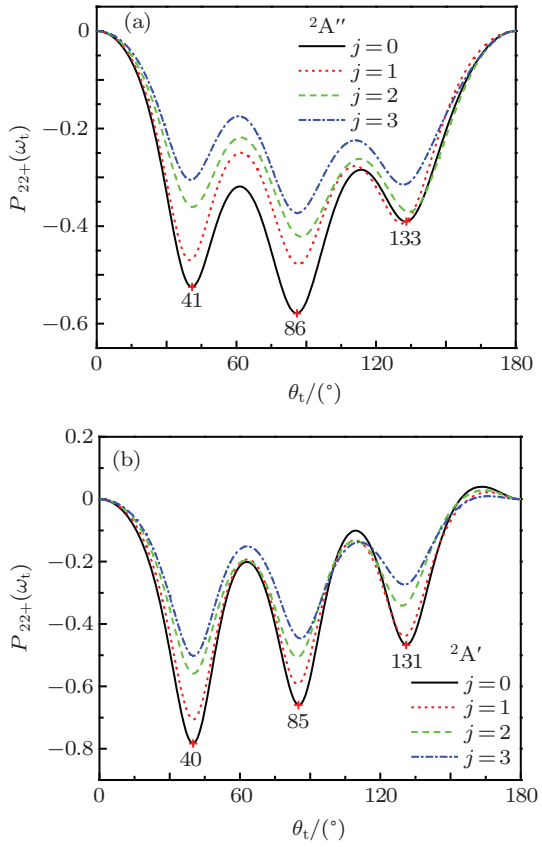


Fig. 6. (color online) Plots of PDDCS $\tilde{P}_{22+}(\omega_t)$ versus θ_t for four reagent rotational excitations at a collision energy of 0.06 eV, based on the ^{2}A″ PES (a) and the ^{2}A′ PES (b).

In the above theoretical calculations, we have neglected the coupling effect between the two PESs, and treated them as separate surfaces. In fact, the linear intermediates (CNO, CON, and NCO) are Renner–Teller molecules, both surfaces (^{2}A″ and ^{2}A′) are degenerate in the linear configurations, and in a fully accurate study they should be coupled through the Renner–Teller interaction. Besides, additional excited $^4\Pi$ surfaces could come into play through non-adiabatic and spin–orbit couplings, and all of them will possibly play an important role in reaction dynamics. However, to our knowledge, at present there is little information about couplings between two surfaces on this reaction.

4. Conclusion

In this paper, the reaction C(^{3}P) + NO(X$^2\Pi$) ($v = 0$, $j = 0 \sim 3$) $\rightarrow$ CN(X$^2\Sigma^+$) + O(^{3}P) is theoretically studied through the QCT approach on two PESs (^{2}A″ and ^{2}A′) at a collision energy of 0.06 eV. Stereodynamics information is obtained for different initial rotational states of reactant NO. Results show that the rotational excitation of the reagent molecule obviously weakens the polarization degree of the rotational angular momentum vector of product CN. Furthermore, we also show QCT calculated PDDCSs on the two PESs, which more clearly illustrates the product rotational angular momentum vectors varying with scattering angle at different rotational states, at three scattering angles they are remarkably polarized. Besides the distribution of $P(\phi_r)$, product polarization varying with the j on the two PESs shows the similar characteristics and change tendencies, which can be ascribed to the similarity between the structures of the two PESs. Compared with the effects of the collision energy,[25] the rotational excitations of the reagent molecule have more considerable influence on the product polarization.

Acknowledgment

Many thanks to Prof. Han Ke-Li for providing the stereodynamics program.

References

[1] Krause H F 1981 *Chem. Phys. Lett.* **78** 78
[2] Dorthe G, Costes M, Naulin C, Joussot-Dubien J, Vaucamps C and Nouchi G 1985 *J. Chem. Phys.* **83** 3171
[3] Sekiya H, Tsuji M and Nishimura Y 1986 *J. Chem. Phys.* **84** 3739
[4] Naulin C, Costes M and Dorthe G 1991 *Chem. Phys.* **153** 519
[5] Dean A J, Hanson R K and Bowman C T 1991 *J. Phys. Chem.* **95** 3180
[6] Costes M, Naulin C, Ghanem N and Dorthe G 1993 *J. Chem. Soc. Faraday Trans.* **89** 1501
[7] Bergeat A, Calvo T, Dorthe G and Loison J C 1999 *Chem. Phys. Lett.* **308** 7
[8] Halvick P, Rayez J C and Evleth E M 1984 *J. Chem. Phys.* **81** 728
[9] Rayez J C, Halvick P, Rayez M T and Duguay B 1986 *Chem. Phys.* **101** 401
[10] Halvick P, Rayez J C, Rayez M T and Duguay B 1987 *Chem. Phys.* **114** 375
[11] Halvick P and Rayez J C 1989 *Chem. Phys.* **131** 375
[12] Wallin E, Elofson P and Holmlid L 1992 *Chem. Phys.* **163** 37
[13] Wallin E, Elofson P and Holmlid L 1994 *Chem. Phys.* **185** 91
[14] Monnerville M, Halvick P and Rayez J C 1993 *J. Chem. Soc. Faraday Trans.* **89** 1579
[15] Simonson M, Marković N, Nordholm S and Persson B J 1995 *Chem. Phys.* **200** 141
[16] Persson B J, Roos B O and Simonson M 1995 *Chem. Phys. Lett.* **234** 382
[17] Beghin A, Stoecklin T and Rayez J C 1995 *Chem. Phys.* **195** 259
[18] Wadi H and Wiesenfeld L 1999 *Chem. Phys. Lett.* **300** 37
[19] Monnerville M, Peoux G, Briquez S and Halvick P 2000 *Chem. Phys. Lett.* **322** 157
[20] Andersson S, Marković N and Nyman G 2000 *Phys. Chem. Chem. Phys.* **2** 613
[21] Andersson S, Marković N and Nyman G 2000 *Chem. Phys.* **259** 99
[22] Abrol R, Wiesenfeld L, Lambert B and Kuppermann A 2001 *J. Chem. Phys.* **114** 7461
[23] Andersson S, Marković N and Nyman G 2003 *J. Phys. Chem. A* **107** 5439
[24] Frankcombe T J and Andersson S 2012 *J. Phys. Chem. A* **116** 4705
[25] Ma J J and Cong S L 2009 *J. At. Mol. Phys.* **26** 1073
[26] Kim S K and Herschbach D R 1987 *Fara. Disc. Chem. Soc.* **84** 159
[27] Case D E, McClelland G M and Heschbach D R 1978 *Mol. Phys.* **35** 541
[28] Shafer-Ray N E, Orr-Ewing A J and Zare R N 1995 *J. Phys. Chem.* **99** 7591
[29] Aoiz F J, Brouard M and Enriquez P A 1996 *J. Chem. Phys.* **105** 4964
[30] Han K L, He G Z and Lou N Q 1996 *J. Chem. Phys.* **105** 8699
[31] Miranda M P and Clary D C 1997 *J. Chem. Phys.* **106** 4509
[32] Aoiz F J, Banares L and Herrero V J 1998 *J. Chem. Soc.,Faraday Trans.* **94** 2483

[33] Miranda M P, Aoiz F J, Bañnares L and Sáez Rábanos V 1999 *J. Chem. Phys.* **111** 5368
[34] Wang M L, Han K L and He G Z 1998 *J. Chem. Phys.* **109** 5446
[35] Chen M D, Wang M L, Han K L and Ding S L 1999 *Chem. Phys. Lett.* **301** 303
[36] Brouard M, Gatenby S D, Joseph D M and Vallance C 2000 *J. Chem. Phys.* **113** 3162
[37] Chen M D, Han K L and Lou N Q 2002 *Chem. Phys. Lett.* **357** 483
[38] Chen M D, Han K L and Lou N Q 2002 *Chem. Phys.* **283** 463
[39] Chen M D, Han K L and Lou N Q 2003 *J. Chem. Phys.* **118** 4463
[40] Ma J J, Chen M D, Cong S L and Han K L 2006 *Chem. Phys.* **327** 529
[41] Ma J J, Zhang Z H and Cong S L 2006 *Acta Phys. Chim. Sin.* **22** 972
[42] Yu Y J, Xu Q and Xu X W 2011 *Chin. Phys. B* **20** 123402
[43] Chen X Q, Wang M S, Yang C L and Wu J C 2012 *Chin. Phys. B* **21** 023402
[44] Xu W W, Liu X G, Luan S X, Sun S S and Zhang Q G 2009 *Chin. Phys. B* **18** 339
[45] Zhang W Q, Cong S L, Zhang C H, Xu X S and Chen M D 2009 *J. Phys. Chem. A* **113** 4192
[46] Liu S L and Shi Y 2011 *Chem. Phys. Lett.* **501** 197
[47] Xu Z H, Zong F J, Han B R, Dong S H, Liu J Q and Ji F 2012 *Chin. Phys. B* **21** 093103
[48] Cheng J, Yue X F and Feng H R 2012 *Chin. Phys. Lett.* **29** 043101
[49] Li R J, Han K L, Li F E, Lu R C, He G Z and Lou N Q 1994 *Chem. Phys. Lett.* **220** 281
[50] Han K L, He G Z and Lou N Q 1989 *Chin. J. Chem. Phys.* **2** 323
[51] Blais N C and Truhlar D G 1977 *J. Chem. Phys.* **67** 1540